Full Paper

Israel Journal of Chemistry

Check for updates

DOI: 10.1002/ijch.202000083

Tuning the Photophysical Properties of Spirolactam Rhodamine Photoswitches

Bo Li,[a] Uroob Haris,[a] Maha Aljowni,[a] Andrew Nakatsuka,[a] Shreya K. Patel,[a, c] and Alexander R. Lippert*[a, b]

Abstract: Spirolactam rhodamines are fluorescent photoswitches that are useful for single molecule localization microscopy, volumetric 3D digital light photoactivatable dye displays, and other applications. Measurement of the photophysical properties, particularly photoswitching kinetics and quantum yields, is challenging and a comprehensive understanding of how molecular structure affects these parameters remains incomplete. In this study, we have synthesized a series of *N*-aryl spirolactam rhodamine photoswitches with fluorescent emissions at 585 nm and 518 nm. Extinction coefficients and fluorescence quantum yields of the fluorescent form of the photoswitch have been measured using excess trifluoroacetic acid to drive the equilibrium to the open form. A method to determine photoswitching kinetics and quantum yields was developed by monitoring the kinetics to reach equilibrium between the on-state and off-state and fitting this data to a rate equation for a reaction in equilibrium. Trends based on the electronic and steric properties of the aryl substituents were evaluated. Using this information, a proof-of-principle demonstration of 3D voxel formation was accomplished using a green (518 nm) emitting photoswitch, setting the foundation for a multi-colour volumetric 3D display.

Keywords: Photoswitches · spirolactam rhodamines · 3D displays · photophysical properties · kinetics

1. Introduction

Photoswitches are molecules that undergo reversible light-mediated isomerization reactions, with the reverse reaction proceeding either thermally or by a second photolytic reaction, often at a different wavelength than the forward reaction.[1] Many classes of photoswitches have been developed and encompass a diverse set of molecular motifs, including azobenzenes,[2] diarylethenes,[3,4] oxazines,[5] acyl hydrazones,[6] spiropyrans,[7] donor-acceptor Stenhouse adducts,[8] indigoids,[9] spirolactam rhodamines,[10] dihydropyrenes,[11] naphthopyrans,[12] dihydroazulenes,[13] and fulgides.[14] In addition to being of fundamental scientific interest, photoswitches have been used for numerous applications, including photopharmacology,[15,16] molecular machines,[17–19] and advanced materials.[20] While these applications rely primarily on shape-dependent features of molecular structures that change upon light illumination, other applications depend on a change in optical properties, including the use of photoswitches in super-resolution microscopy[21] and volumetric 3D displays.[22,23] Microscopy and optical display applications depend on photoswitches that can be transformed from a non-fluorescent off-state into a fluorescent on-state upon illumination with a specific wavelength of light. This fluorescent on-state can then be excited to the emissive fluorescent excited state by illumination with the same or a different wavelength of light. Rapid relaxation to the non-fluorescent off-state is usually a spontaneous thermal process for super-resolution microscopy and 3D display applications, but this can also be achieved by a photolytic process.

Spirolactam rhodamines are an important class of fluorescent photoswitches that have found widespread use in single molecule localization microscopy[24–27] and 3D displays.[22] Gleiter et al. first demonstrated that *N*-aryl spirolactam rhodamines adopt a colourless, non-fluorescent closed form (off-state, Figure 1A), but upon illumination with ultraviolet light, a photochemical reaction occurs which transforms the molecule from the closed lactam form into an open fluorescent form (on-state, Figure 1A) that persists for milliseconds to minutes depending on the solvent medium.[28] Later, the same group explored the kinetics of the colouring reaction and thermal fading in mixed solvents of dioxane with water or alcohols.[29] Thermal isomerization rates and activation vol-

---

[a] B. Li, U. Haris, M. Aljowni, A. Nakatsuka, S. K. Patel, A. R. Lippert
Department of Chemistry
Southern Methodist University
3215 Daniel Avenue, Dallas, TX 75206 USA
E-mail: alippert@smu.edu
[b] A. R. Lippert
Center for Drug Discovery
Design and Delivery (CD4)
Southern Methodist University
Dallas, TX 75206 USA
[c] S. K. Patel
Department of Chemistry and Biochemistry
University of California, Los Angeles
607 Charles E. Young Drive East
Los Angeles, CA 90095-1569 USA

Supporting information for this article is available on the WWW under https://doi.org/10.1002/ijch.202000083

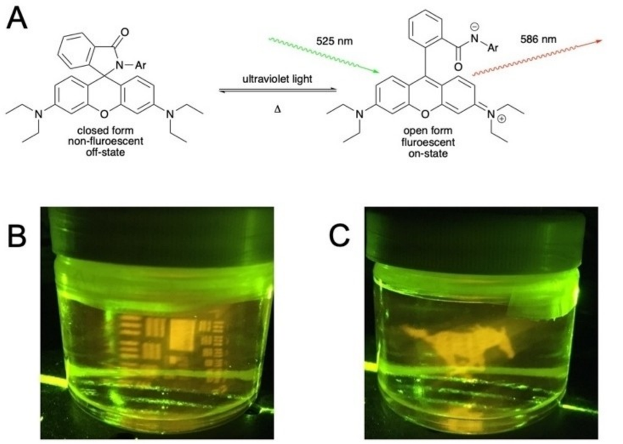

Figure 1. Photoswitching of *N*-aryl spirolactam rhodamines for use in a volumetric 3D digital light photoactivatable dye display (3D Light PAD). (A) Photoswitching of *N*-phenyl spirolactam rhodamine B. (B) Resolution chart projected in a 3D Light PAD. (C) SMU Peruna projected in a 3D Light PAD.

umes were also investigated by Sueishi and coworkers,[30] and the influence of rotameric isomers of the on-state were postulated to explain the observed effects of solvent and pressure. Bossi et al. further explored the kinetics of isomerization and acidophotochromism in the presence of trifluoroacetic acid for *N*-phenyl spirolactam rhodamine and several derivatives.[31] They proposed a four-state mechanism to explain the acid-dependent photoswitching behaviour, and used a mathematical model to extract kinetic parameters. The acid-dependent properties of *N*-phenyl spirolactam rhodamine and its derivatives have been explored independently by Scott and Harbron, and these properties make molecules of this type useful as fluorometric pH probes.[32–35] The above studies have been aided by advanced synthetic methodology for the synthesis of a wide variety of spirolactam rhodamine derivatives.[10,24,32–35]

Despite progress in understanding the kinetics of photoswitching for *N*-phenyl spirolactam rhodamine derivatives, determining the photochemical parameters, particularly photoswitching rate constants and quantum yields, remains difficult. This difficulty has impeded understanding of molecular structure-function relationships for spirolactam rhodamine B photoswitches and full photophysical measurements have not been performed in dichloromethane. In our previous work,[22] we used *N*-phenyl spirolactam rhodamine B as a fluorescent photoswitch to generate 3D images in a solution of dichloromethane in a 3D display that we call a volumetric 3D digital light photoactivatable dye display (3D Light PAD, Figures 1B, C). In this display, a solution of *N*-phenyl spirolactam rhodamine B in dichloromethane containing 7.2 μM triethylamine is prepared and placed in an imaging chamber with glass or quartz walls. An ultraviolet light projector is used to photoactivate the spirolactam rhodamine photoswitch in a precise pattern, which then intersects with a visible light pattern generated with a visible light projector. Fluorescence only occurs where the UV and visible light patterns intersect, making it possible to produce free-floating volumetric 3D images such as the resolution chart shown in Figure 1B and the SMU Peruna Mustang shown in Figure 1C.

In order to better understand the design principles of spirolactam rhodamine photoswitches and ultimately generate photoswitches of different colours that would be suitable for use in a 3D Light PAD, we synthesized and measured the photophysical properties of a range of *N*-aryl spirolactam rhodamine B (SRB) photoswitches with red (585 nm) emission wavelengths and *N*-aryl spirolactam rhodamine derivatives with fluorinated aminoalkyl groups (SRCF3) that have green (518 nm) emission wavelengths. Herein, we report the synthesis of these derivatives, including a new procedure to prepare fluorinated spirolactam rhodamine derivatives, and present a method to measure the kinetics and quantum yields of the photoswitching process. This information is used to provide a preliminary demonstration of 3D voxel formation using a green emitting spirolactam rhodamine photoswitch in a 3D Light PAD display.

2. Experimental Section

2.1 Synthetic Procedures

2.1.1 General Materials and Methods

All reactions were performed in dried glassware under an atmosphere of dry N_2. Silica gel P60 (SiliCycle) was used for column chromatography and SiliCycle 60 F254 silica gel (precoated sheets, 0.25 mm thick) was used for analytical thin layer chromatography. Plates were visualized by fluorescence quenching under UV light or by staining with iodine. Other reagents were purchased from Sigma-Aldrich (St. Louis, MO), Alfa Aesar (Ward Hill, MA), EMD Millipore (Billerica, MA), or Oakwood Chemical (West Columbia, SC) and used without further purification. ^{1}H NMR and ^{13}C NMR spectra for characterization of new compounds and monitoring reactions were collected in $CDCl_3$ (Cambridge Isotope Laboratories, Cambridge, MA) on a JEOL 500 MHz spectrometer or Bruker 400 MHz spectrometer in the Department of Chemistry at Southern Methodist University. All chemical shifts are reported in the standard notation of parts per million using the peak of residual proton signals of the deuterated solvent as an internal reference. Coupling constant units are in Hertz (Hz). Splitting patterns are indicated as follows: br, broad; s, singlet; d, doublet; t, triplet; q, quartet; m, multiplet; dd, doublet of doublets; dt, doublet of triplets. High resolution mass spectroscopy was performed on a Shimadzu IT-TOF (ESI source) at the Shimadzu Center for Advanced Analytical Chemistry at the University of Texas, Arlington. Low resolution mass spectrometry was performed using an Advion Expression^L CMS (ESI source) at Southern Methodist University. Complete synthetic details can be found in the Supporting Information.

2.1.2 Representative Procedure for Fluorinated N-Aryl Spirolactam Rhodamine (SRCF3) Compounds

3-oxo-3H-spiro[isobenzofuran-1,9′-xanthene]-3′,6′-diyl bis (trifluoromethanesulfonate) (bis-triflate).[36] Fluorescein (2.79 g, 8.42 mmol, 1.0 equiv.) and bis(trifluoromethanesulfonyl) aniline (7.52 g, 21.1 mmol, 2.5 equiv.) were dissolved in dichloromethane (20 mL). Then, diisopropylethylamine (4.31 mL, 25.2 mmol, 3.0 equiv.) was added into the mixture. The reaction mixture was allowed to stir at 25 °C for 18 h. The reaction was monitored by thin layer chromatography (TLC). After the reaction was complete, the mixture was diluted with 20 mL dichloromethane, washed with 1 M HCl (3 × 20 mL), 1 M $NaHCO_3$ (3 × 20 mL), and then washed with brine. The organic layer was collected, dried over Na_2SO_4, filtered, and concentrated under reduced pressure. The crude product was purified by silica gel chromatography with dichloromethane: methanol (20 : 1) as the eluent, affording the product as a light yellow solid (3.56 g, 71 % yield). ^{1}H NMR (500 MHz, $CDCl_3$) 8.05 (d, J = 7.0 Hz, 1H), 7.73–7.69 (m, 2H), 7.29 (s, 2H), 7.19 (d, J = 6.6 Hz, 1H), 7.01–6.97 (m, 4H).

3′,6′-bis((2,2,2-trifluoroethyl)amino)-3H-spiro[isobenzofuran-1,9′-xanthen]-3-one (Rhodamine-CF_3). The pure bis-triflate (2.98 g, 5.04 mmol, 1 equiv.) was added into a 50 mL pressure flask with $Pd_2(dba)_3$ (462 mg, 0.504 mmol, 0.1 equiv.), XPhos (720 mg, 1.51 mmol, 0.3 equiv.) and Cs_2CO_3 (4.60 g, 14.1 mmol, 2.8 equiv.). The flask was evacuated under high vacuum for 10 min and filled with N_2. The mixture was then dissolved in 20 mL dioxane and stirred for 15 min under N_2. 2,2,2-trifluoroethylamine (0.92 mL, 12.9 mmol, 2.4 equiv.) was added into the mixture by dropwise addition. The flask was capped and heated at 100 °C for 20 h. The mixture was then transferred into a round bottom flask and the solvent was evaporated. The residue was dissolved in ethyl acetate and poured into brine (50 mL), 1 M HCl (10 mL) was added, and the mixture was extracted with ethyl acetate (3 × 25 mL). The organic layer was collected, dried over Na_2SO_4, filtered, and concentrated under reduced pressure. The crude product was purified by silica gel chromatography with dichloromethane:methanol (30 : 1) as the eluent, affording the product as a red solid (1.59 g, 64 % yield). ^{1}H NMR (500 MHz, $CDCl_3$) 7.99 (m, 1H), 7.65 (m, 1H), 7.59 (m, 1H), 7.17 (d, 1H), 6.58 (s, 2H), 6.51 (m, 2H), 6.36 (t, J = 8.3 Hz, 2H), 4.23 (br s, 2H), 3.78 (m, 4H). ^{13}C NMR (125 MHz, $CDCl_3$) 167.7, 154.8, 154.0, 133.3, 131.9, 130.6, 128.7, 123.9, 108.7, 98.1, 69.3, 44.6, 37.9, 30.0, 14.9, 12.6. HRMS calculated for $C_{24}H_{16}N_2O_3F_6$ $[M+H]^+$ 495.1121, found 495.1119.

2-phenyl-3′,6′-bis((2,2,2-trifluoroethyl)amino)spiro[isoindoline-1,9′-xanthen]-3-one (10). Rhodamine-CF3 (305 mg, 0.607 mmol, 1.0 equiv.) and aniline (0.19 mL, 1.82 mmol, 3.0 equiv.) were dissolved in dichloromethane (10 mL). The mixture was cooled to 0 °C, then $POCl_3$ (0.07 mL, 0.73 mmol, 1.2 equiv.) was added dropwise. The reaction mixture was allowed to stir at 0 °C for 15 min and then heated to 45 °C for 20 h. The mixture was diluted with 10 mL dichloromethane and then washed with 1 M HCl (3 × 10 mL), 1 M NaOH (3 × 10 mL), and brine. The organic layer was collected, dried over Na_2SO_4, filtered, and concentrated under reduced pressure. The crude product was purified by silica gel chromatography with ethyl acetate : hexane (1 : 4) as the eluent, affording the product as a white solid (221.4 mg, 62 % yield). The compound can be additionally purified by recrystallization from ethyl acetate:hexanes (1 : 2) to provide a spectroscopically pure sample ^{1}H NMR (500 MHz, $CDCl_3$) 8.01 (d, J = 7.1 Hz, 1H), 7.54–7.50 (m, 2H), 7.14–7.08 (m, 4H), 6.65 (d, J = 8.0 Hz, 4H), 6.30 (d, J = 8.6 Hz, 4H), 3.73 (q, J = 6.6 Hz, 4H). ^{13}C NMR (125 MHz, $CDCl_3$) 167.6, 152.7, 147.0, 135.9, 132.9, 131.3, 129.1, 127.3, 126.2, 123.7, 110.3, 99.3, 67.1, 45.9, 29.7. HRMS calculated for $C_{30}H_{21}N_3O_2F_6$ $[M+H]^+$ 570.1533, found 570.1531.

2.2 Determination of Photophysical Properties

2.2.1 Extinction Coefficients of the On-State and Off-State, $\varepsilon_{556nm(on)}$, $\varepsilon_{495nm(on)}$, $\varepsilon_{254nm(off)}$

Stock solutions (0.5 mM) of recrystallized *N*-aryl spirolactam rhodamine B (SRB) derivatives **1**–**9** or *N*-aryl spirolactam rhodamine derivatives with fluorinated aminoalkyl groups (SRCF3) **10**–**17** were prepared in dichloromethane. A 25 mM stock solution of trifluoroacetic acid in dichloromethane was prepared for use with the SRB derivatives and a 250 mM stock solution of trifluoroacetic acid was prepared for use with the SRCF3 derivatives. For the SRB derivatives, the SRB stock solutions and trifluoroacetic acid stock solutions were diluted into 1 mL quartz cuvettes to prepare five solutions of the SRB derivative with final concentrations between 1 μM and 30 μM, each containing 50 equivalents of trifluoroacetic acid. The capped cuvettes were allowed to sit for 40 minutes to ensure complete reaction to the fluorescent on-form. A similar procedure was used for the SRCF3 derivatives, except that 500 equivalents of trifluoroacetic acid were used. After complete conversion, UV/Visible absorbance spectra were acquired for each concentration and the extinction coefficient was determined using the slope of the linear plot of concentration versus absorbance at 556 nm for the SRB derivatives and 495 nm for the SRCF3 derivatives according to Beer's law. A similar procedure was used to determine the extinction coefficient at 254 nm of the off-state, but in the absence of any trifluoroacetic acid. All values are the average of n = 3 independent experiments ± standard deviation. More details can be found in the supporting information.

2.2.2 Fluorescence Quantum Yield of the On-State, Φ_{fl}

Fluorescence quantum yields were determined in dichloromethane solutions of SRB with the addition of 50 equivalents of trifluoroacetic acid and SRCF3 with the addition of 500 equiv.alents of trifluoroacetic acid using rhodamine B as a standard. Five solutions of the standard rhodamine B were prepared in ethanol to have absorbance values between 0.01 and 0.1. The absorbance was measured at 550 nm and integrated fluorescence emission was measured using an excitation wavelength of 550 nm. A similar procedure was used to prepare five solutions of the SRB and SRCF3 derivatives, measuring the absorbance and exciting the fluorescence at 556 nm for the SRB derivatives and measuring the absorbance and exciting the fluorescence at 495 nm for the SRCF3 derivatives. The quantum yield was determined by using equation 1, where G is the slope of the linear plot of integrated fluorescence emission versus absorbance, G_{stand} is the slope of the same plot for the standard, η is the index of refraction for the sample solutions, approximated as the index of refraction of dichloromethane (1.42) and η_{stand} is the index of refraction of the standard solution, approximated as the index of refraction of ethanol (1.36). Φ_{fl} is the fluorescence quantum yield of the sample and $\Phi_{stand} = 0.5$, the fluorescence quantum yield of the standard, rhodamine B in ethanol.[37] All values are the average of $n = 3$ independent experiments ± standard deviation.

$$\Phi_{fl} = \Phi_{stand} \times \frac{G}{G_{stand}} \times \frac{\eta^2}{\eta^2_{stand}} \qquad (1)$$

2.2.3 Determination of k_{off}, k_{on}, and K_{eq}

Kinetics were determined using fluorescence spectroscopy. Samples of SRB and SRCF3 were prepared at 5 µM in dichloromethane in a quartz cuvette and placed in a Hitachi F-7000 fluorescence spectrophotometer. For the SRB derivatives, the following parameters were used: $\lambda_{ex} = 254$ nm, $\lambda_{em} = 585$ nm, excitation slits = 5 nm, emission slits = 2.5 nm. For the SRCF3 derivatives, the following parameters were used: $\lambda_{ex} = 254$ nm, $\lambda_{em} = 518$ nm, excitation slits = 5 nm, emission slits = 5 nm. Kinetic scans were performed with continuous excitation at 254 nm until an equilibrium was reached, 100 seconds to 30 minutes, depending on the compound. The 254 nm illumination both initiates photochemical conversion from the off-state to the on-state and excites fluorescence of the on-state. The traces were then fit to an equation for a reaction in equilibrium, equation 2, where I_{fl} is the observed fluorescence emission (proportional to the concentration of the on-state), I_{max} is the theoretical maximum emission with complete turn-on of the dye, k_{on} is the rate constant for the forward reaction, k_{off} is the rate constant for the reverse reaction, and B is a parameter to account for non-zero background signal. Fitting was performed using Mathematica 12.0, with all parameters constrained to be positive. Values for I_{max} were estimated by measuring the fluorescence emission of 1 or 10 upon addition of excess trifluoroacetic acid, and these estimates were used to constrain the value of I_{max}. This constraint was found to be critical to provide consistent values of k_{on}. K_{eq} was determined as k_{on}/k_{off}. All values are the averages from fitting of $n = 3$ independent experiments ± standard deviation, except for compounds 5 and 6, which were the average values from fitting $n = 6$ independent experiments. Equation 2 is derived in the supporting information.

$$I_{fl} = I_{max} \times \frac{k_{on}}{k_{on} + k_{off}} \times (1 - e^{-(k_{on} + k_{off})t}) + B \qquad (2)$$

2.2.4 Determination of the Photochemical Quantum Yield for Photoswitching to the On-State, Φ_{pc}

The photochemical quantum yields Φ_{pc} were determined using equation 3,[38] where k_{on} is the rate of conversion to the on-state as determined by fitting equation 2, ε_{254nm} is the extinction coefficient of the off-state at 254 nm, V is the volume of the solution (0.3 mL), I_0 is the intensity of the excitation light at 254 nm (50.8 $\mu W\,cm^{-2}$, measured with a Digital Light Meter, ThorLabs PM100D), and l is the path length of the cuvette (1 cm). All values are the average of $n = 3$ independent experiments ± standard deviation.

$$\Phi_{pc} = \frac{k_{on} V}{I_0\, \varepsilon_{254nm}\, l \ln 10} \qquad (3)$$

3. Results and Discussion

We became interested in spirolactam rhodamine photoswitches due to photoswitching properties that make them ideal for use in a volumetric 3D digital light photoactivatable dye display (3D Light PAD): a non-fluorescent off-state, a fluorescent on-state, fast UV photoactivated switching, and fast thermal relaxation.[22] While these properties enabled the development of a first generation monochrome 3D Light PAD, optimization and expansion into multi-colour displays requires a thorough understanding of the photoswitching design parameters and how molecular structure affects these parameters. These include the extinction coefficients of the off-state at the ultraviolet photoactivation wavelength ($\varepsilon_{254nm(off)}$) and of the on-state at the fluorescence excitation wavelength ($\varepsilon_{556nm(on)}$, $\varepsilon_{495nm(on)}$), the fluorescence quantum yield of the on-state (Φ_{fl}), the photochemical quantum yield for the photoactivation reaction (Φ_{pc}), and the on and off kinetic rate constants for photoswitching (k_{on}) and thermal relaxation (k_{off}). Factors such as solubility, stability, and toxicity are also important for

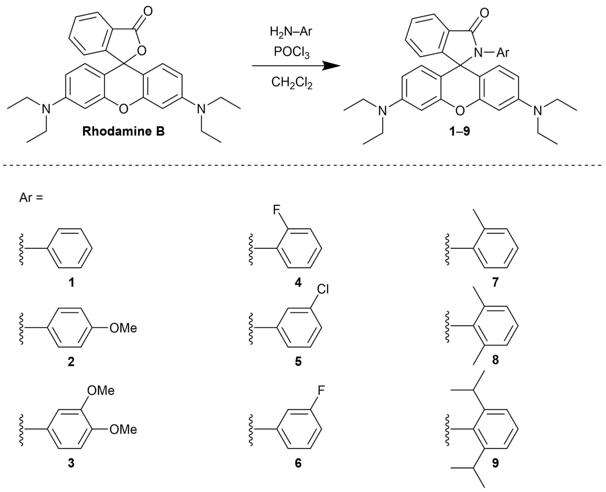

Figure 2. Synthesis of SRB derivatives.

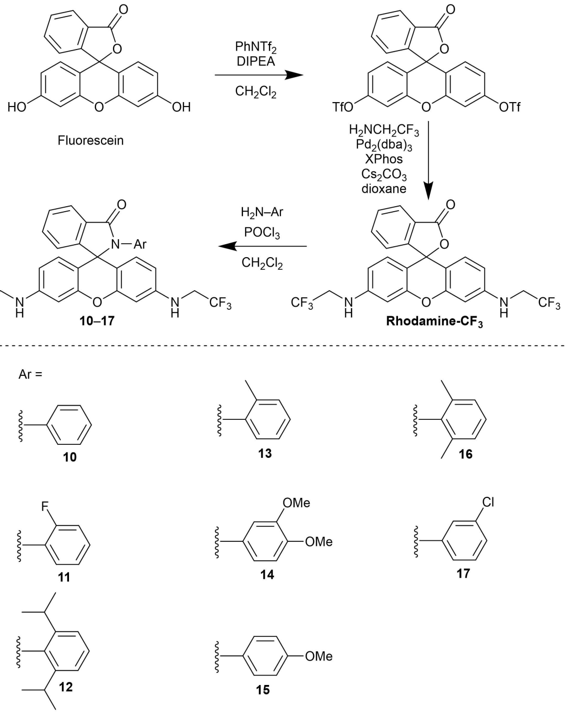

Figure 3. Synthesis of SRCF3 derivatives.

eventual commercialization of a 3D display of this type, but these parameters are not considered in the current study.

Ideally, the on-rate should be fast and is dependent on the extinction coefficient of the off-form of the photoswitch at the photoactivation wavelength ($\varepsilon_{254nm(off)}$), the excitation light intensity (I_0), and the photochemical quantum yield (Φ_{pc}), as described by equation 3.[38] Additionally, the off-rate should be fast to avoid diffusion of the on-form of the dye, which generates blurry images. The brightness of the display depends on the extinction coefficient at the visible excitation wavelength of the on-form of the dye ($\varepsilon_{556nm(on)}$, $\varepsilon_{495nm(on)}$) and the fluorescence quantum yield (Φ_{fl}), as well as the concentration of the on-form of the photoswitch at equilibrium (K_{eq}). Blue-shifting the emission wavelength of the on-form of the photoswitch can be accomplished by fluorination,[10] but the effect that this has on the parameters described above and how to modify the molecular structure to optimize these parameters is unclear. In order to investigate these factors, we decided to generate a library of derivatives by varying the *N*-aryl groups and investigate if tuning this position could provide an avenue towards new photoswitches for use in a volumetric 3D display.

We synthesized nine spirolactam rhodamine B (SRB) derivates and eight fluorinated spirolactam rhodamine (SRCF3) derivatives. The SRB derivatives were prepared from rhodamine B using a phosphorus oxychloride mediated coupling with a library of anilines (Figure 2).[32–35] Derivatives were chosen to explore electron-rich aryl groups (compounds **2**, **3**, **7**–**9**), electron-poor aryl groups (compounds **4**–**6**), and steric hindrance at the photoswitchable spirolactam motif (compounds **7**–**9**). We identified fluorinated spirolactam rhodamines containing trifluoroethylamino groups as a photoswitch with green fluorescence emission at 518 nm.[24,25] We experienced difficulty constructing the xanthene core using the fluorinated aminophenol according to the literature precedent,[24,25] so we decided to devise an alternative streamlined synthetic route to prepare these compounds using recently developed Buchwald-Hartwig coupling conditions (Figure 3).[36] Starting from fluorescein, the bis-triflate can be prepared in good yield using *N*-phenyl bis-triflimide as a triflating reagent. The bis-triflate can then be coupled to trifluoroethylamine under palladium catalysis using the XPhos ligand to generate the fluorinated rhodamine derivative with trifluorethylamino groups. The same phosphorus oxychloride amide coupling reaction that was used to prepare the spirolactam rhodamine B (SRB) derivatives can be used to prepare the fluorinated spirolactam rhodamine (SRCF3) derivatives. Here again, we prepared derivatives with electron-rich aryl groups (Compounds **12**–**16**), electron-poor aryl groups (Compounds **11**, **17**), and sterically-hindered groups (Compounds **12**, **13**, **16**).

With these compounds in hand, we first measured the extinction coefficients ($\varepsilon_{556nm(on)}$, $\varepsilon_{495nm(on)}$) and fluorescence quantum yields (Φ_{fl}) of the on-form of the dyes. We capitalized on the light-independent, acid-mediated switching of these compounds,[32–35] and determined that we could convert the dyes completely to the on-form with the addition of 50 equivalents of trifluoroacetic acid for the SRB photoswitch series and 500 equivalents of trifluoroacetic acid for SRCF3 photoswitch series, each measured after a 40 minute incubation time (Figure S2). Using this method, we determined extinction coefficients at 556 nm for the on-state of the SRB photoswitch series (Table 1) and at 495 nm for the SRCF3 series (Table 2). For the SRB series, extinction coefficients were found to be between 84,700 and 132,100, while for the SRCF3 series, extinction coefficients were found to be between 54,400 and

Table 1. Fluorescence quantum yields and extinction coefficients of the on-state of *N*-aryl spirolactam rhodamine B (SRB) derivatives in dichloromethane.

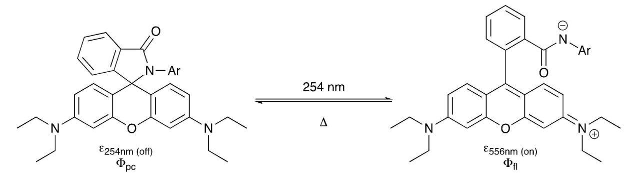

Compound	Φ_{fl}/%	$\varepsilon_{556nm(on)}$
1	52	84,700
2	5	122,400
3	16	110,200
4	36	96,000
5	24	118,900
6	55	132,100
7	15	117,500
8	28	103,500
9	33	112,200

94,900. The fluorescence quantum yields (Φ_{fl}) were also determined in the presence of excess trifluoracetic acid to drive the equilibrium into the open form. Generally, quantum yields were lower for derivatives with electron-rich aryl groups (compounds **2**, **3**, **7**, **13**–**15**), likely due to photoinduced electron transfer (PET) quenching.[39] Interestingly, derivatives that were electron-rich, but also had high steric hindrance at the spirolactam motif (compounds **8**, **9**, **12**, **16**) showed fluorescence quantum yields that were not as attenuated. We hypothesize that this could be due to a deviation from planarity reducing conjugation between the aryl group and amide, and subsequently reducing PET quenching. While supported by a trend of increased quantum yield as the steric hindrance increases from compound **7** (2-methyl) to compound **8** (2,6-dimethyl) to compound **9** (2,6-diisopropyl), further investigation would be needed to confirm this.

We next sought to determine the on-rates (k_{on}) and photochemical quantum yields (Φ_{pc}) of the photoswitching reactions. The on-rates and photochemical quantum yields are related according to equation 3 and depend on the extinction coefficients of the off-form ($\varepsilon_{254nm(off)}$) and the excitation light intensity (I_0). Our approach was to measure the fluorescence emission at the emission maximum of the on-form upon continuous excitation at 254 nm and then fit this data to the rate equation for a reaction at equilibrium, equation 2 (Figure 4). The 254 nm excitation light served to both mediate the photochemical reaction from the off-state to the on-state and excite the fluorescence of the on-state. We began by formulating methods using *N*-phenyl spirolactam rhodamine B, compound **1**. We found that monitoring fluorescence emission at 585 nm upon continuous excitation at 254 nm provided a curve that reached an equilibrium value after approximately 1000 seconds (Figure 4A). A digital light meter was used to measure the light intensity, which was found to be 50.8 μW cm^{-2}. We note that there is a non-zero fluorescence signal at the initial time point, likely due to light scattering and a non-zero fluorescence of the off-state when excited at the ultraviolet 254 nm wavelength. This background is accounted for by adding a background parameter, B, into the mathematical fits.

Table 2. Fluorescence quantum yields and extinction coefficients of the on-state of fluorinated *N*-aryl spirolactam rhodamine (SRCF3) derivatives in dichloromethane.

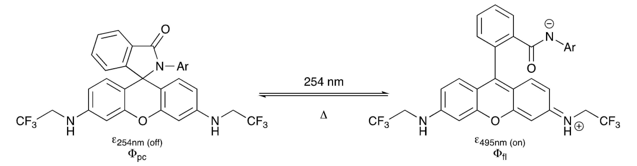

Compound	Φ_{fl}/%	$\varepsilon_{495nm(on)}$
10	58	94,900
11	24	91,400
12	41	94,200
13	6	90,900
14	3	65,900
15	1	58,900
16	31	70,300
17	13	54,400

The data in this experiment was fit to equation 3 and, in a representative fit, the rate constants were determined as k_{on} =

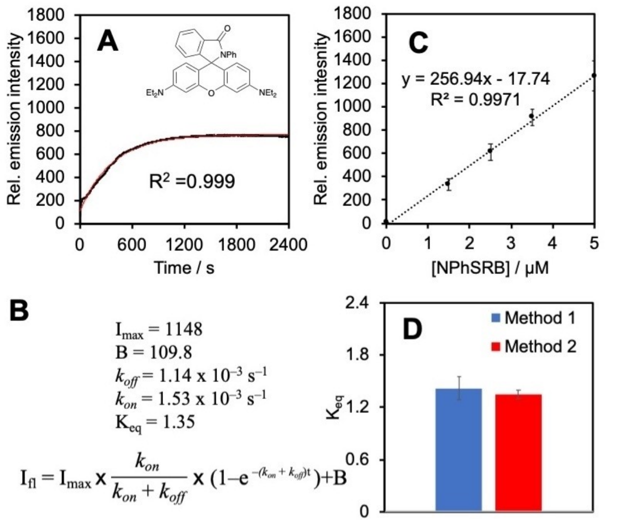

Figure 4. Methodology to measure photoswitching rates. (A) Emission intensity at 585 nm of 5 μM **1** in CH_2Cl_2 irradiated with 50.8 μW cm^{-2} of 254 nm light (black trace) and the fit to equation 3 (red trace). (B) Equation and parameters found for the trace shown in (A). (C) Calibration curve generated from increasing concentrations of **1** in CH_2Cl_2 40 min after addition of 50 equivalents of TFA. Data are average values from n = 6 independent experiments. Error bars are ± S.D. (D) Comparison of K_{eq} determined from Method 1: k_{off} and k_{on} found from equation 1 and Method 2: Determined by evaluating the equilibrium concentration of the on-state using the equilibrium fluorescence emission in (A) and the calibration curve in (C).

$1.53 \times 10^{-3}\,s^{-1}$, $k_{off} = 1.14 \times 10^{-3}\,s^{-1}$ (Figure 4B). These values allowed us to determine an equilibrium constant of $K_{eq} = 1.4$. It is important to note that the fitted parameters, particularly k_{on}, are sensitive to the constraints placed on the maximum intensity (I_{max}). In order to confirm these fits and provide reasonable constraints on the I_{max}, we compared the equilibrium constant determined with this fit to the equilibrium constant determined by estimating the maximum turn-on value (I_{max}) by addition of excess trifluoracetic acid to drive the equilibrium to the on-state (Figure 4C). In Figure 4C, the 5 μM concentration data point on this calibration curve represents an estimate of the maximum fluorescence (I_{max}) if the photoswitch is completely in the open fluorescent form. The calibration curve in Figure 4C can be used to determine the concentration of the fluorescent on-form once the photochemical reaction reaches equilibrium by comparing the equilibrium fluorescence emission in Figure 4A to the calibration curve in Figure 4C. The equilibrium constant determined by these two methods is similar (Figure 4D), increasing confidence in this approach. The addition of trifluoracetic acid to estimate the maximum fluorescence emission of **1** for SRB derivatives and **10** for SRCF3 derivatives was used in all following measurements to provide reasonable constraints on I_{max} and more reliable measures of k_{on}.

We fitted the fluorescence turn-on data and determined photochemical quantum yields for the series of SRB photoswitches (Table 3). Extinction coefficients ($\varepsilon_{254nm(off)}$) were determined at 254 nm for the off-form of the dyes in dichloromethane and were found to be between 34,500 and 47,000. The off-rates, k_{off}, were determined to be in the range of 0.38–$6.1 \times 10^{-3}\,s^{-1}$ for the SRB photoswitch series. Generally, SRB photoswitches with electron-poor aryl groups (2-fluoro, 3-chloro, and 3-fluoro, compounds **4**–**6**) and the very sterically hindered 2,6-diisopropyl compound **9** had lower values for k_{off} between 0.38–$0.72 \times 10^{-3}\,s^{-1}$. On the other hand, electron-rich aryl groups (4-methoxy, 3,4-dimethoxy, 2-methyl, and 2,6-dimethyl, compounds **2**, **3**, **7** and **8**) had similar or higher values for k_{off} as the parent *N*-phenyl SRB **1** between 0.93–$6.1 \times 10^{-3}\,s^{-1}$. The k_{off} values determined for the 4-methoxy and 3,4-dimethoxy derivatives **2** and **3** were elevated to 1.4–$6.1 \times 10^{-3}\,s^{-1}$, consistent with these electron donating substituents pushing the equilibrium towards the closed form of the photoswitch. The k_{off} values were plotted versus the Hammett parameters of the substituents to show a reasonable trend with a negative ρ value (Figure S6).

We next evaluated the k_{on} values and used these to determine the equilibrium constant (K_{eq}) of the photostationary state and the photochemical quantum yield for the photoswitching reaction (Φ_{pc}). While the 4-methoxy and 3,4-dimethoxy electron-rich derivatives **2** and **3** have lower k_{on}, Φ_{pc}, and K_{eq}, consistent with a preference for the closed form in these structures, the effect of electron withdrawing and sterically hindered substituents on k_{on} was less pronounced. Compared to the electron-rich compounds **2** and **3**, we generally do observe higher k_{on} and Φ_{pc} for the phenyl, 2-fluoro, 2-methyl, 2,6-dimethyl, and 2,6-diisopropyl compounds **1**, **4**, **7**, **8**, and **9**, indicating that steric hindrance at the spirolactam unit can increase the photoswitching on-rate and quantum yield of photoactivation. However, the 2-fluoro, 3-chloro, and 3-fluoro derivatives **4**–**6** all display k_{on} and Φ_{pc} values slightly lower than the parent phenyl derivative **1**, indicating that the photochemical reaction rate k_{on} is less strictly dependent on the electronic nature of the *N*-aryl substituent. We also performed similar analyses of the *N*-phenyl spirolactam rhodamine B **1**, but in the presence of 7.2 μM triethylamine, as is used in the operation of the 3D Light PAD.[22] While other parameters remained relatively constant, addition of triethylamine had a dramatic effect on the k_{off} value, which increases from $1.2 \times 10^{-3}\,s^{-1}$ in the absence of triethylamine to $30 \times 10^{-3}\,s^{-1}$ in the presence of triethylamine. This 30-fold increase in the off-rate is consistent with our preliminary evaluation[22] and helps explain the better image quality observed when triethylamine is added to the solution.

Table 3. Kinetics and photochemical quantum yields of 5 μM *N*-aryl spirolactam Rhodamine B (SRB) derivatives in dichloromethane.

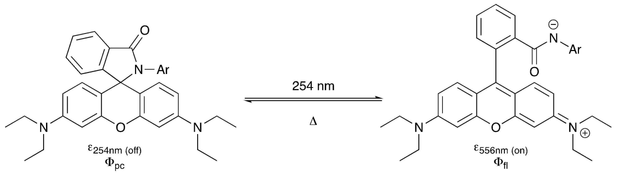

Compound	$\varepsilon_{254nm(off)}$	K_{eq}	k_{off}[a]	k_{on}[a]	Φ_{pc}/%
1	40,300	1.4 ±0.05	1.2 ±0.3	1.6 ±0.4	6.0 ±1.5
2	42,600	0.044 ±0.023	6.1 ±3.5	0.31 ±0.26	1.1 ±0.93
3	41,800	0.17 ±0.056	1.4 ±0.44	0.25 ±0.14	0.82 ±0.45
4	40,400	1.5 ±0.12	0.72 ±0.16	1.1 ±0.2	4.1 ±0.83
5[b]	47,000	1.2 ±0.15	0.38 ±0.24	0.49 ±0.34	1.6 ±1.1
6[b]	42,300	1.9 ±0.62	0.57 ±0.45	0.97 ±0.54	3.1 ±1.8
7	41,300	1.6 ±0.13	0.93 ±0.56	1.5 ±1.0	6.7 ±3.7
8	34,500	0.68 ±0.14	2.7 ±1.1	1.8 ±1.0	8.0 ±4.2
9	38,900	1.4 ±0.46	0.60 ±0.1	0.84 ±0.39	3.3 ±1.5
1[c]	40,300[d]	0.009 ±0.007	30 ±27	1.7 ±0.28	5.5 ±0.89

[a] Values are $10^{-3}\,s^{-1}$ [b] n = 6 independent experiments [c] in the presence of 7.2 μM triethylamine [d] $\varepsilon_{254nm(off)}$ of **1** in CH_2Cl_2

Next, we measured these parameters for the newly synthesized SRCF3 photoswitch series. In general, we found that the values for the off-rates, k_{off}, were much higher for these derivatives in comparison to the SRB derivatives, and values as high as 180–$360 \times 10^{-3}\,s^{-1}$ were measured for the phenyl, 3,4-dimethoxy, and 4-methoxy compounds **10**, **14**, and **15** (Table 4). This is consistent with the fluorination of the amino groups inductively shifting the equilibrium to prefer the

Table 4. Kinetics and photochemical quantum yields of 5 µM fluorinated *N*-aryl spirolactam rhodamine (SRCF3) derivatives in dichloromethane.

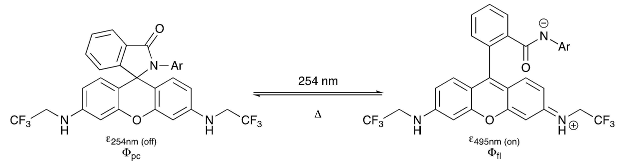

Compound	$\varepsilon_{254nm(off)}$	K_{eq}	k_{off} [a]	k_{on} [a]	Φ_{pc}/%
10	41,300	0.016 ±0.001	180 ±26	2.9 ±0.29	11 ±1
11	37,600	0.28 ±0.051	4.7 ±1.4	1.3 ±0.26	5.3 ±1.0
12	36,500	0.75 ±0.038	2.8 ±1.1	2.1 ±0.79	8.8 ±3.3
13	40,400	0.094 ±0.064	3.2 ±1.2	0.25 ±0.066	0.94 ±0.002
14	36,300	0.0095 ±0.001	290 ±16	2.7 ±0.47	11 ±2.0
15	41,100	0.0094 ±0.002	360 ±88	3.3 ±0.9	18 ±5.0
16	36,800	0.78 ±0.10	1.9 ±0.086	1.5 ±0.14	6.1 ±0.56
17	43,400	0.069 ±0.008	46 ±19	3.1 ±0.89	11 ±3.1

[a] Values are $10^{-3}\,s^{-1}$

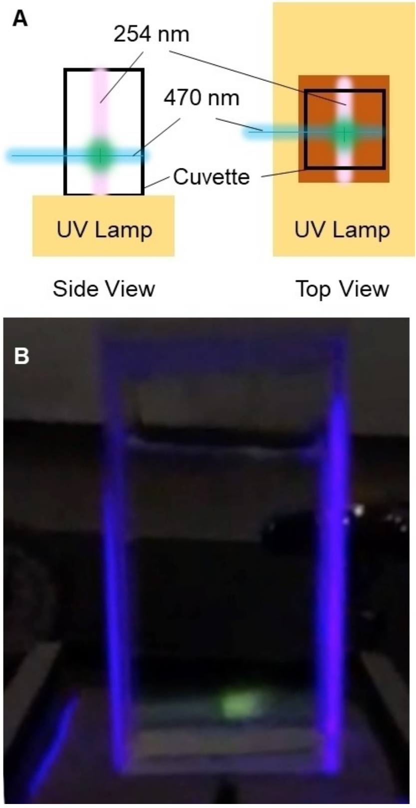

Figure 5. Demonstration of 3D Voxel Formation. (A) Schematic and (B) photograph of the setup for 3D voxel formation using a 254 nm TLC lamp, the blue LED of a LightCrafter 4500 projector, and a cuvette filled with 5 µM **11** and 7.2 µM triethylamine.

closed conformation of the dye. This effect could be overcome by introducing electron-withdrawing 2-fluoro and 3-chloro groups (compound **11** and **17**) or steric hinderance at the spirolactam position (2,6-diisopropyl, 2-methyl, and 2,6-dimethyl, compounds **12**, **13**, **16**), which display slower k_{off} values between $1.9–4.7\times10^{-3}\,s^{-1}$ for compounds **11**–**13**, **16** and $46\times10^{-3}\,s^{-1}$ for the 3-chloro compound **17**. On the other hand, we found that the k_{on} values and photochemical quantum yields were slightly higher for SRCF3 derivatives versus SRB derivatives, but showed less predictable trends across different types of SRCF3 derivatives.

Finally, we used the information gathered from these experiments to do a preliminary demonstration of 3D voxel formation with green emission using the design principles of a 3D Light PAD. We used the 2-fluoro SRCF3 compound **11** in dichloromethane and a 254 nm excitation source. The photoswitch was dissolved at 5 µM in dichloromethane with 7.2 µM triethylamine in a 2.5 cm × 2.5 cm × 5 cm cuvette. A mask was constructed to place over a 254 nm TLC lamp so that a line of UV light would project up from the TLC lamp into the cuvette (Figure 5A). A square of blue light was projected from the side using a LightCrafter 4500 projector. Using this setup, a voxel of green light can be observed (Figure 5B), providing a proof-of-principle demonstration for using green SRCF3 photoswitches in a 3D Light PAD. Unfortunately, photoactivation was only efficient at 254 nm, so patterning could not be achieved using the commercially available WinTech 4500 UV projector (as used in our previous work),[22] which is equipped with a 385 nm LED.

4. Conclusions

In summary, we have successfully synthesized a series of fluorescent spirolactam rhodamine photoswitches with fluorescence emission in the red (585 nm) or green (518 nm) portion of the spectrum. We report measurements of extinction coefficients, fluorescence and photochemical quantum yields, and kinetics of photoswitching. The strengths of the study include a useful new synthetic protocol to synthesize SRCF3 photoswitches using a Buchwald-Hartwig coupling with trifluoroethylamine. The reported method to measure photochemical quantum yields and photoswitching kinetics is useful because it does not require ultrafast methods and can be performed using fluorescence spectrophotometers that are readily available. These parameters have been difficult to measure and photoswitching parameters in dichloromethane solvent were previously unavailable in the literature. This study provides important insights into how molecular structure of *N*-aryl spirolactam rhodamine derivatives affects the photoswitching properties, with identification of steric hindrance at the spirolactam motif and electronics of the *N*-aryl groups as being key design principles for tuning photoswitch behaviour.

We do note some important limitations of the study. While it was found that the off-rate, k_{off}, was generally very robust in the kinetic fitting, the fits for the on-rate, k_{on} (and consequently quantum yields Φ_{pc}) were dependent on the constraints given for the I_{max} parameter, which correlates with the maximum fluorescence emission of the photoswitch in its fully on-state. While we performed experiments using excess trifluoroacetic acid to provide estimates of the magnitude of the I_{max} emission in the fully on-state, these measurements should be interpreted carefully.

In the future, detailed studies of the trends and confirmation of the switching rates and quantum yields may be approachable using time-resolved spectroscopy techniques. Additionally, we have reported a number of new photoswitchable fluorescent spirolactam rhodamine molecules that could find use in super-resolution imaging methodology, including single molecule localization microscopy. We have demonstrated 3D voxel formation, but implementation into a 3D display capable of generating more complex images would require either further tuning of derivatives to be more excitable using 385 nm optics in currently available projectors or the development of new projectors with optics capable of patterning light in the deeper UV region centred at 254 nm. Furthermore, this technology could find use in volumetric 3D printing applications that are currently being explored by various groups, including our own.

Acknowledgements

The authors acknowledge the American Chemical Society Petroleum Research Fund (60759-ND1) and Southern Methodist University for supporting this project (start-up funds to A. R.L. and a University Research Council Grant). A.R.L. discloses a financial stake in BioLum Sciences, LLC, a company developing point-of-care medical devices.

References

[1] Z. L. Pianowski, *Chem. Eur. J.* **2019**, *25*, 5128–5144.
[2] A. A. Beharry, G. A. Woolley, *Chem. Soc. Rev.* **2011**, *40*, 4422–4437.
[3] M. Irie, T. Fukaminato, K. Matsuda, S. Kobatake, *Chem. Rev.* **2014**, *114*, 12174–12277.
[4] Z. Li, C. He, Z. Lu, P. Li, Y. P. Zhu, *Dyes Pigm.* **2020**, *182*, 108623.
[5] Y. Zhang, S. Tang, E. R. Thapaliya, L. Sansalone, F. M. Raymo, *Chem. Commun.* **2018**, *54*, 8799–8809.
[6] B. Shao, H. Qian, Q. Li, I. Aprahamian, *J. Am. Chem. Soc.* **2019**, *141*, 8364–8371.
[7] R. Klajn, *Chem. Soc. Rev.* **2014**, *43*, 148–184.
[8] S. Helmy, F. A. Leibfarth, S. Oh, J. E. Poelma, C. J. Hawker, J. Read de Alaniz, *J. Am. Chem. Soc.* **2014**, *136*, 8169–8172.
[9] C. Petermayer, H. Dube, *Acc. Chem. Res.* **2018**, *51*, 1153-1163.
[10] V. N. Belov, M. L. Bossi, *Isr. J. Chem.* **2013**, *53*, 267–279.
[11] K. Klaue, W. Han, P. Liesfeld, F. Berger, Y. Garmshausen, S. Hecht, *J. Am. Chem. Soc.* **2020**, *142*, 11857–11864.
[12] Y. Inagaki, Y. Kobayashi, K. Mutoh, J. Abe, *J. Am. Chem. Soc.* **2017**, *139*, 13429–13441.
[13] S. L. Broman, M. B. Nielsen, *Phys. Chem. Chem. Phys.* **2014**, *16*, 21172–21182.
[14] Y. Yokoyama, *Chem. Rev.* **2000**, *100*, 1717–1740.
[15] M. M. Lerch, M. J. Hansen, G. M. van Dam, W. Symanski, B. L. Feringa, *Angew. Chem. Int. Ed. Engl.* **2016**, *55*, 10978–10999.
[16] K. Hüll, J. Morstein, D. Trauner, *Chem. Rev.* **2018**, *118*, 10710–10747.
[17] I. Aprahamian, *ACS Cent. Sci.* **2020**, *6*, 347–358.
[18] J. F. Stoddart, *Angew. Chem. Int. Ed. Engl.* **2017**, *56*, 11094–11125.
[19] B. L. Feringa, *Angew. Chem. Int. Ed. Engl.* **2017**, *56*, 11060–11078.
[20] A. Goulet-Hanssens, F. Eisenreich, S. Hecht, *Adv. Mater.* **2020**, *32*, 1905966.
[21] F. M. Jradi, L. D. Lavis, *ACS Chem. Biol.* **2019**, *14*, 1077–1090.
[22] S. K. Patel, J. Cao, A. R. Lippert, *Nat. Commun.* **2017**, *8*, 15239.
[23] S. Wan, H. Zhou, J. Lin, W. Lu, *Angew. Chem. Int. Ed. Engl.* **2020**, *59*, 8416–8420.
[24] V. N. Belov, M. L. Bossi, J. Fölling, V. P. Boyarskiy, S. W. Hell, *Chem. Eur. J.* **2009**, *15*, 10762–10776.
[25] G. Y. Mitronova, V. N. Belov, M. L. Bossi, C. A. Wurm, L. Meyer, R. Medda, G. Moneron, S. Bretschneider, C. Eggeling, S. Jakobs, S. W. Hell, *Chem. Eur. J.* **2010**, *16*, 4477–4488.
[26] M. K. Lee, P. Rai, J. Williams, R. J. Twieg, W. E. Moerner, *J. Am. Chem. Soc.* **2014**, *136*, 14003–14006.
[27] E. A. Halabi, D. Pinotsi, P. Rivera-Fuentes, *Nat. Commun.* **2019**, *10*, 1232.
[28] K. H. Knauer, R. Gleiter, *Angew. Chem. Int. Ed. Engl.* **1977**, *16*, 113.
[29] H. Willwohl, J. Wolfrum, R. Gleiter, *Laser Chem.* **1989**, *10*, 63–72.
[30] Y. Sueishi, Y. Sugiyama, S. Yamamoto, N. Nishimura, *J. Phys. Org. Chem.* **1993**, *6*, 478–482.
[31] H. Montenegro, M. Di Paolo, D. Capdevila, P. F. Aramendía, M. L. Bossi, *Photochem. Photobiol. Sci.* **2012**, *11*, 1081–1086.
[32] W. L. Czaplyski, G. E. Purnell, C. A. Roberts, R. M. Allred, E. J. Harbron, *Org. Biomol. Chem.* **2014**, *12*, 526-533.
[33] Q. A. Best, C. Liu, P. D. van Hoveln, M. E. McCarroll, C. N. Scott, *J. Org. Chem.* **2013**, *78*, 10134–10143.
[34] C. Liu, Q. A. Best, B. Suarez, J. Pertile, M. E. McCarroll, C. N. Scott, *J. Fluoresc.* **2015**, *25*, 231–237.
[35] S. G. Stratton, G. H. Taumoefolau, G. E. Purnell, M. Rasooly, W. L. Czaplyski, E. J. Harbron, *Chem. Eur. J.* **2017**, *23*, 14064–14072.
[36] J. B. Grimm, L. D. Lavis, *Org. Lett.* **2011**, *13*, 6354–6357.
[37] T. Karstens, K. Kobs, *J. Phys. Chem.* **1980**, *84*, 1871–1872.
[38] B. Shao, M. Baroncini, H. Qian, L. Bussotti, M. Di Donato, A. Credi, I. Aprahamian, *J. Am. Chem. Soc.* **2018**, *140*, 12323–12327.
[39] Y. Urano, M. Kamiya, K. Kanda, T. Ueno, K. Hirose, T. Nagano, *J. Am. Chem. Soc.* **2005**, *127*, 4888–4894.

Manuscript received: September 30, 2020
Revised manuscript received: November 4, 2020
Version of record online: ■■, ■■

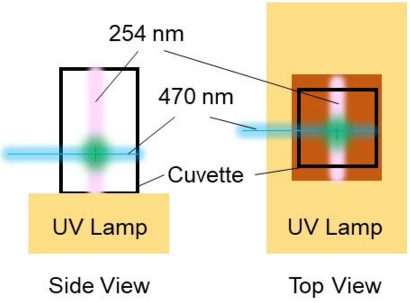

*B. Li, U. Haris, M. Aljowni, A. Nakatsuka, S. K. Patel, A. R. Lippert**

1 – 10

Tuning the Photophysical Properties of Spirolactam Rhodamine Photoswitches